

# Catalysis Science & Technology

Accepted Manuscript



This is an *Accepted Manuscript*, which has been through the Royal Society of Chemistry peer review process and has been accepted for publication.

*Accepted Manuscripts* are published online shortly after acceptance, before technical editing, formatting and proof reading. Using this free service, authors can make their results available to the community, in citable form, before we publish the edited article. We will replace this *Accepted Manuscript* with the edited and formatted *Advance Article* as soon as it is available.

You can find more information about *Accepted Manuscripts* in the [Information for Authors](#).

Please note that technical editing may introduce minor changes to the text and/or graphics, which may alter content. The journal's standard [Terms & Conditions](#) and the [Ethical guidelines](#) still apply. In no event shall the Royal Society of Chemistry be held responsible for any errors or omissions in this *Accepted Manuscript* or any consequences arising from the use of any information it contains.

Cite this: DOI: 10.1039/c0xx00000x

www.rsc.org/xxxxxx

ARTICLE TYPE

# Mesoporous zirconium phosphonate materials as efficient water-tolerable solid acid catalysts

Xiu-Zhen Lin<sup>a</sup>, Tie-Zhen Ren<sup>b</sup> and Zhong-Yong Yuan<sup>\*a</sup>

Received (in XXX, XXX) Xth XXXXXXXXX 20XX, Accepted Xth XXXXXXXXX 20XX

DOI: 10.1039/b000000x

Mesoporous organic-inorganic hybrid zirconium phosphonate materials (ZrHEDP, ZrATMP and ZrEDTMPS) with organic groups bridged in the frameworks are synthesized by using 1-hydroxyethylidene-1,1'-diphosphonic acid (HEDP), amino tri(methylene phosphonic acid) (ATMP) and sodium salt of ethylene diamine tetra(methylene phosphonic acid) (EDTMPS) as the coupling molecules, respectively, in the presence of surfactant cetyltrimethylammonium bromide. The obtained hybrid mesostructures exhibited high surface area of 310 – 749 m<sup>2</sup>/g, uniform pore size of 3.4 – 4.2 nm and large pore volume of 0.42 – 0.74 cm<sup>3</sup>/g, as well as H<sup>+</sup> exchange capacity of 1.25 – 1.92 mmol/g, which are catalytically active for ethyl acetate hydrolysis in aqueous medium and for water-produced acetic acid esterifications of ethanol or cyclohexanol. These water-tolerable solid acid catalysts possess superior stability, as revealed by four-time recycling in the cyclohexanol esterification of acetic acid with well retained textural properties and acid active sites. The well preservation of active acid sites on the pore surfaces of the prepared mesoporous zirconium phosphonate hybrid materials is related with the hydrophobic nature of organic groups integrated in the hybrid framework.

## 1. Introduction

As important functional materials, solid acid catalysts have become even more important for petroleum industry and for environmental-friendly fine chemicals production with respect to non-corrosiveness, safety, waste minimization and ease of separation and recovery.<sup>1-4</sup> Since a large amount of reactions such as hydrolysis and dehydration are related to water as reactant or product, water-tolerable solid acid catalysts are more preferable.<sup>5-7</sup> Among the reported solid acid catalysts,<sup>8,9</sup> poor thermal stability of ion-exchange resins,<sup>10,11</sup> small pore sizes of zeolites<sup>8,12</sup> and non-negligible aqueous solubility of heteropolyacids<sup>13-15</sup> largely restrict their widespread applications. Although a series of transition metal (mainly Zr(IV)) phosphates have been considered as ideal candidates for water-related reactions due to their desirable water-resistance ability and high thermal stability,<sup>9,16</sup> their catalytic performance was not high enough for practical applications, because of inadequate hydrophobicity on the pore surface contributing to the acid active sites easily deactivated after surrounded by water.

Metal phosphonate materials are promising non-siliceous inorganic-organic hybrids that are synthesized by combining metal joints and organophosphonic linkages at the molecular scale, attracting great attention in the fields including acid catalysis.<sup>17,18</sup> One of the great advantages of this kind of materials as solid acid lies in the fact that they are ready to be precisely tailored for functionalization purposes, since versatile organophosphonate groups could be utilized to adjust their interfacial hydrophobic/hydrophilic properties<sup>19,20</sup> and allow for

the control of both reactivity and selectivity of organic reaction process. Additionally, as the derivatives of inorganic metal phosphates, metal phosphonate hybrids possess some attractive aspects of the former including desirable insolubility and good sedimentation that are favourable for water-related reactions. Piermatti and co-workers synthesized alkyl and/or aryl phosphonate-modified zirconium hydrogen phosphate with general formula Zr(PO<sub>3</sub>OH)<sub>2-(x+y)</sub>(PO<sub>3</sub>R)<sub>x</sub>(PO<sub>3</sub>R<sup>1</sup>)<sub>y</sub> as efficient heterogeneous Brønsted acid catalysts for aza-Diels-Alder reaction in aqueous medium,<sup>21</sup> and the L-proline-functionalized analogues were active in the direct asymmetric aldol addition of cyclohexanone to *p*-nitrobenzaldehyde in sole water, due to hydrophobic groups bearing on organophosphorus pendant on solid surface.<sup>22</sup> Segawa and Ozawa reported that composited zirconium phosphonate Zr[(O<sub>3</sub>PCH<sub>2</sub>SO<sub>3</sub>H)<sub>x</sub>(-O<sub>3</sub>PC<sub>12</sub>H<sub>25</sub>)<sub>1-x</sub>]<sub>2</sub> exhibited better catalytic activity than single analogue Zr[(O<sub>3</sub>PCH<sub>2</sub>SO<sub>3</sub>H)<sub>x</sub> in esterification of acetic acid, due to the extra hydrophobic function (-C<sub>12</sub>H<sub>25</sub>).<sup>19</sup> These materials were all prepared based on ZrO<sub>2</sub> inorganic frameworks that had been grafted with monophosphonate bearing the hydrophobic organic groups, possessing low surface area and poor porosity.

Recently, a series of high-surface-area mesoporous metal phosphonate materials with the homogeneous incorporation of different organic groups in the framework were reported by using organically bridged polyphosphonic acids and their derivatives (e.g. salts or esters) as coupling molecules, demonstrating their multifunctionality and application potential in sustainable energy and environment.<sup>23,24</sup> Remarkably, the inherent acidity from dissociative P-OH groups (also called uncoordinated or defective

P-OH) endows them to be outstanding acid catalysts and ion exchangers.<sup>25</sup> The hydroxyethylidene-bridged mesoporous zirconium phosphonates exhibited high catalytic activity with rapid reaction rate for the synthesis of methyl-2,3-O-isopropylidene- $\beta$ -D-ribofuranoside from D-ribose.<sup>26</sup> However, the effect of the organic groups on the acid-catalytic performance of mesoporous metal phosphonate materials was little mentioned to date.

In this paper, a series of mesoporous zirconium phosphonates were synthesized by a facile surfactant-assistant method with the use of claw-type coupling molecules of 1-hydroxy ethylidene-1,1'-diphosphonic acid (HEDP), amino tri(methylene phosphonic acid) (ATMP) and ethylene diamine tetra(methylene phosphonic acid) (EDTMP), possessing favourable surface area and uniform pore size. The organic groups beared on the organophosphonates were integrated in the hybrid framework, but not pendent on the inorganic network. HEDP, ATMP and EDTMPS with different chain length of organic groups were selected with the aim to investigate the role of internal organic groups played in the catalytic activity. The water-tolerable catalytic properties of the prepared materials were evaluated, and the water-related reactions of ethyl acetate hydrolysis, esterification of acetic acid with ethanol or cyclohexanol were selected as testing reactions.

## 2. Experimental

### 2.1 Materials

Zirconium oxychloride ( $\text{ZrOCl}_2 \cdot 8\text{H}_2\text{O}$ ), cetyltrimethylammonium bromide (CTAB), cyclohexanol and ethyl acetate were purchased from Tianjin Guangfu Fine Chemical Research Institute. HEDP (60 wt%), ATMP (50 wt%) and sodium salt of ethylene diamine tetra(methylene phosphonic acid) (EDTMPS, 30 wt%) were donated from Henan Qingyuan Chemical Co. Strong-acidic ion-exchange resin NKC-9 was obtained from the Chemical Plant of Nankai University, and  $\text{H}_3\text{PO}_4$  was from Tianjin Huadong Reagent Plant. All chemicals were used as received without further purification.

### 2.2 Catalyst preparation

In a typical synthesis of mesoporous zirconium phosphonates, 1.82 g of CTAB was solved in 20 ml of deionized water, followed by addition of 1.72 g of HEDP or 3.0 g of ATMP or 4.5 g of EDTMPS under stirring at 45 °C. Because EDTMPS was in sodium salt instead of acid form, extra HCl (2 mol/L) was added to adjust the pH value of above mixture to 2. After 2 h of stirring, the mixed solution of 0.3–0.8 g of zirconium oxychloride and 5 ml of deionized water was added dropwise into the above solution and continued to stir overnight. The final molar ratio of HEDP :  $\text{ZrOCl}_2$  : CTAB was 5.4 : 1 : 5.4 (P/Zr = 10.8), ATMP :  $\text{ZrOCl}_2$  : CTAB was 2 : 1 : 2 (P/Zr = 6), and EDTMPS :  $\text{ZrOCl}_2$  : CTAB was 0.89 : 1 : 2 (P/Zr = 3.5). The resulting gel containing HEDP was transferred into a Teflon-lined autoclave and heated at 110 °C for 24 h, while the gel with ATMP or EDTMPS was stirred for another 36 h at 75 °C. The white solid products were filtered, washed with water and dried under vacuum at 80 °C for 6 h, and denoted as ZrHEDP, ZrATMP and ZrEDTMPS for the samples synthesized with HEDP, ATMP and EDTMPS, respectively. The surfactant embedded in the product was removed by extraction with HCl/ethanol solution, namely, 1 g of

sample in 150 ml of ethanol with 3.6 ml of con. HCl under 60 °C stirred for 8 h.

For the sake of comparison, mesoporous zirconium phosphate (denoted as  $\text{ZrPO}_4$ ) was also synthesized. 0.063 g of  $\text{H}_3\text{PO}_4$ , 2 g of CTAB and 15 ml of  $\text{H}_2\text{O}$  were mixed under stirring for 2 h at 45 °C to form transparent solution. An aqueous solution of 0.87 g  $\text{ZrOCl}_2$  in 5 ml of  $\text{H}_2\text{O}$  was added dropwise, and the mixture was stirred for another 36 h. The solid was collected by filtering, washing with a large amount of water, and drying at 100 °C, followed by calcination at 550 °C for 5 h with a heating rate of 2 °C/min from room temperature to 550 °C to remove the involved CTAB species.

### 2.3 Characterization

The chemical compositions of Zr and P were analyzed by inductively coupled plasma (ICP) emission spectroscopy on a Thermo Jarrell-Ash ICP-9000 (N+M) spectrometer. X-ray diffraction (XRD) patterns were recorded on a Bruker D8 Focus diffractometer with  $\text{Cu K}\alpha$  radiation, operated at 40 kV and 40 mA.  $\text{N}_2$  adsorption-desorption isotherms were recorded on a Quantachrome NOVA 2000e sorption analyzer at liquid nitrogen temperature (77 K). The samples were degassed at 120 °C for at least 6 h prior to the measurement. The surface areas were calculated by multi-point Brunauer-Emmett-Teller (BET) method, and the pore size distributions were calculated from the adsorption branch of the isotherms by Barret-Joyner-Halenda (BJH) method and the non-local density functional theory (NLDFT). Temperature programmed desorption (TPD) measurements were conducted on a Quantachrome ChemBET 3000 analyzer. Transmission electron microscopy (TEM) was carried out on a FEI Tecnai G20 microscope at 200 kV. Thermogravimetry (TG) analysis was performed on a TA SDT Q600 instrument under air atmosphere at a heating rate of 5 °C/min using  $\alpha\text{-Al}_2\text{O}_3$  as the reference. Fourier transform infrared (FT-IR) spectra were measured on a Bruker VECTOR 22 spectrometer with KBr pellet technique, and the ranges of spectrograms were 4000 to 400  $\text{cm}^{-1}$ . Solid state  $^{31}\text{P}$  (161.8 MHz) MAS (magic angle spinning) NMR (nuclear magnetic resonance) spectra and  $^{13}\text{C}$  (100.5 MHz) CP/MAS NMR spectra were measured on a Varian Infinity Plus-400 spectrometer. The chemical shift of  $^{31}\text{P}$  MAS NMR spectra was referenced to 85%  $\text{H}_3\text{PO}_4$ .

The acid content of mesoporous zirconium organophosphonates and ion exchange resin NKC-9 was determined from the titration curve. 0.1 g of catalyst was stirred with 20 ml of 10 wt% NaCl solution at room temperature for 12 h and filtrated. Then 0.05 M NaOH was used to titrate the acidic content of the filtrate.

The acidity of  $\text{ZrPO}_4$  was studied by  $\text{NH}_3$ -TPD. About 200 mg of sample was placed in a U-shaped sample tube, pre-treated in helium (20 ml/min) at 200 °C for 30 min and then cooled to 100 °C. With that ammonia was adsorbed on the samples for 30 min. The physisorbed ammonia was removed by flushing the sample with helium for 1 h. TPD measurements were carried out in the temperature range of 100 – 900 °C.

### 2.4 Catalytic testing

Hydrolysis of ethyl acetate (HEA) was carried out by heating an aqueous solution of ethyl acetate (8.5 g, 5 wt%) to 80 °C in a

glass vial (5 ml). 0.1 g of the solid acid catalyst was added to the solution to initiate the reaction. The catalytic activity was then measured by gas chromatograph (GC) analysis of the solution after 2 h.

In the esterification of acetic acid with ethanol (EAE), 0.2 g of catalyst and 5.0 ml of acetic acid (0.087 mol) were added into a three-necked round flask equipped with a condenser and a magnetic stirrer. After the temperature rising to 80 °C, 21.0 ml of ethanol (0.356 mol) was rapidly added, and the reaction was continued for 5 h. In this reaction, the molar ratio of ethanol/acetic acid was 4.0, and the mass ratio of catalyst/acetic acid was 0.038. The product was ethyl acetate with selectivity of near 100%, determined by GC analysis.

Esterification of acetic acid with cyclohexanol (EAC) was performed by mixing and stirring 0.2 g of catalyst and 11.5 ml of cyclohexanol (0.117 mol) in a three-necked round flask equipped with a condenser and a magnetic stirrer. After heating the mixture to 100 °C by oil bath, 17.5 ml of acetic acid (0.306 mol) was rapidly added and the reaction was continued for 10 h. In this reaction, the molar ratio of acetic acid/cyclohexanol was 2.6 and the mass ratio of catalyst/cyclohexanol was 0.017. The product was cyclohexyl acetate with selectivity of near 100%, determined by GC analysis.

### 3. Results and discussion

#### 3.1 Material synthesis and characterization

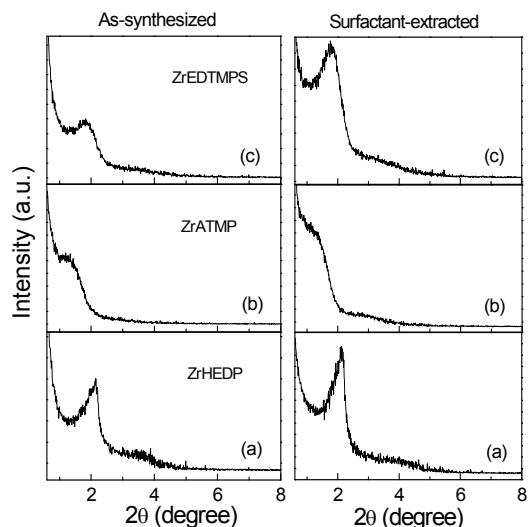
The synthesis of mesoporous zirconium phosphonates was conducted in the presence of surfactant CTAB with the use of HEDP, ATMP and EDTMPS as organophosphorus coupling molecules, as shown in Scheme S1 (ESI†). The surfactant removal from the pores of the as-prepared samples was carried out by extraction in HCl/ethanol solution, not pure ethanol solution. This is because the cationic CTA<sup>+</sup> from CTAB connected with negative charged species such as RPO<sub>3</sub><sup>-</sup> or Zr-O<sup>-</sup> from the hybrid backbone based on charge interaction, and positive charged species such as H<sup>+</sup> were needed to keep charge balance of the hybrid framework when the CTA<sup>+</sup> left, which is similar with the surfactant-removal mechanism proposed for siliceous materials.<sup>27,28</sup> The compositions of the prepared materials were investigated by ICP and CHN analysis due to inorganic and organic components, and the results were summarized in Table 1. The P/Zr molar ratios in the hybrid framework for the prepared samples were in the range of 2.68–3.45, which are less than those in the synthesis gels (3.5–10.6).

Fig. 1 shows the low-angle XRD patterns of the obtained zirconium organophosphonate samples before and after surfactant-removal. The as-synthesized samples ZrHEDP, ZrATMP and ZrEDTMPs showed main reflections at 2–2.5°, 1.2–1.7° and 1.7–2.2° (2θ), respectively, besides very weak and broad peaks in the 2θ range of 3–4°, indicating the feature of mesostructure. Due to the ill-resolved reflections in 3–4° (2θ), their exact mesophases can not be well defined yet. After the acidic ethanol extraction process, the relative intensities of the diffraction peaks strengthened due to the removal of surfactant, while their positions were not shifted much, suggesting that the surfactant removal did not cause pore contraction of the mesostructures.

**Table 1** Elemental compositions of the as-synthesized hybrid materials containing surfactant, and their corresponding formula.

sample	C (%)	H (%)	N (%)	P/Zr ratio <sup>a</sup>	Formula
ZrHEDP	24.43	5.1	1.18	3.31 (10.6)	Zr <sub>2</sub> (HEDP) <sub>3.31</sub> ·1.5CTAB·5.2H <sub>2</sub> O
ZrATMP	24.85	4.57	2.76	3.45 (6.0)	ZrATMP <sub>1.15</sub> ·0.6CTAB·7.1H <sub>2</sub> O
ZrEDTMPs	26.48	5.88	3.8	2.68 (3.5)	Zr <sub>1.5</sub> EDTMPs·0.7CTAB·8.4H <sub>2</sub> O

<sup>a</sup> The value in parenthesis was the P/Zr molar ratio in the synthetic gel.



**Fig. 1** Low-angle XRD patterns of as-synthesized and surfactant-extracted samples: (a) ZrHEDP, (b) ZrATMP and (c) ZrEDTMPs.

N<sub>2</sub> adsorption-desorption isotherms of the synthesized mesoporous zirconium phosphonates and their corresponding pore size distribution curves are shown in Fig. 2. The isotherms of all three hybrid samples are similar to each other and present two stages. The first stage at relative pressure  $P/P_0 < 0.5$  is of type IV and the second stage at  $P/P_0 > 0.5$  is of type II with H3 hysteresis loop, demonstrating the presence of uniform mesopores together with the secondary pores from the particle aggregation.<sup>29</sup> At the first stage with relative pressure  $P/P_0 < 0.5$ , an increase in N<sub>2</sub> volume was observed at  $P/P_0 = 0.22$ – $0.38$  for ZrHEDP,  $0.4$ – $0.5$  for ZrATMP, and  $0.25$ – $0.4$  for ZrEDTMPs. The shift of sharp increase step in N<sub>2</sub> adsorption towards higher relative pressure for the three samples implied their corresponding increase in mesopore size. The pore size distribution curves calculated by the NLDFT model show narrow pore size distributions centered at 3.4, 4.2 and 3.6 nm for ZrHEDP, ZrATMP and ZrEDTMPs, respectively. The BET surface area of 749 m<sup>2</sup>/g and pore volume of 0.74 cm<sup>3</sup>/g are obtained for ZrHEDP, 310 m<sup>2</sup>/g and 0.42 cm<sup>3</sup>/g for ZrATMP, and 670 m<sup>2</sup>/g and 0.67 cm<sup>3</sup>/g for ZrEDTMPs, respectively, which are rather appreciable. The previously reported porous zirconium phosphonates synthesized by means of surfactant-assisted strategy with the use of benzenephosphonate,<sup>30</sup> 1-phosphomethylproline<sup>31</sup> and 1,4-bis(phosphomethyl)piperazine<sup>32</sup> provided low specific surface areas (usually below 350 m<sup>2</sup>/g) with wide pore size distributions. Jia et al.<sup>33</sup> and Veliscek-Carolan et al.<sup>34</sup> prepared ZrATMP in the absence of surfactants, but with very poor porosity, indicating the effect of surfactant

templating during the formation of mesophases. Table 2 listed the textural properties of the synthesized hybrids.

**Table 2** Textural properties and  $H^+$  exchange capacities of the catalysts, and their catalytic results in esterifications of acetic acid with ethanol (EAE), esterification of acetic acid with cyclohexanol (EAC) and hydrolysis of ethyl acetate (HEA).

Samples	$S_{BET}$ ( $m^2/g$ )	$V_{pore}$ ( $cm^3/g$ )	$D_{DFT}$ (nm)	$D_{BJH}$ (nm)	Acid content (mmol $H^+$ /g)	EAE		EAC		HEA	
						Yield (%)	TOF <sup>c</sup>	Yield (%)	TOF <sup>d</sup>	Yield (%)	Per acidic protons (mmol/mol <sub>acid</sub> /min)
ZrHEDP	749	0.74	3.4	2.3	1.92	67.5	152.9	76.8	234.0	10.2	21.5
ZrHEDP <sup>a</sup>	650	0.67	3.1	2.1	2.0						
ZrATMP	310	0.42	4.2	3.3	1.25	52.6	183.0	65.4	306.1	9.5	30.6
ZrATMP <sup>a</sup>	259	0.31	3.6	2.8	1.71						
ZrEDTMPS	670	0.67	3.6	2.6	1.42	66.9	204.9	75.3	310.2	18.0	51.1
ZrEDTMPS <sup>a</sup>	602	0.61	3.1	2.3	1.58						
ZrPO <sub>4</sub>	282	0.33	2.6–14	1.5	2.03 <sup>b</sup>	54.3	116.4	72.9	210.1	7.6	15.1
ZrPO <sub>4</sub> <sup>a</sup>	260	0.32	2.4–16	1.4	1.95 <sup>b</sup>						
NKC-9	12	0.02	1.9	—	4.33	88.1	88.5	87.9	118.7	37.9	35.2
NKC-9 <sup>a</sup>	11	0.02	1.9	—	3.49						

<sup>a</sup> Materials recycled four times in the esterification of acetic acid with cyclohexanol. <sup>b</sup> Acidity of the catalyst measured by  $NH_3$ -TPD. <sup>c</sup> TOF is based on mmol of acetyl acetate/mmol of active site. <sup>d</sup> TOF is based on mmol of cyclohexyl acetate/mmol of active site.

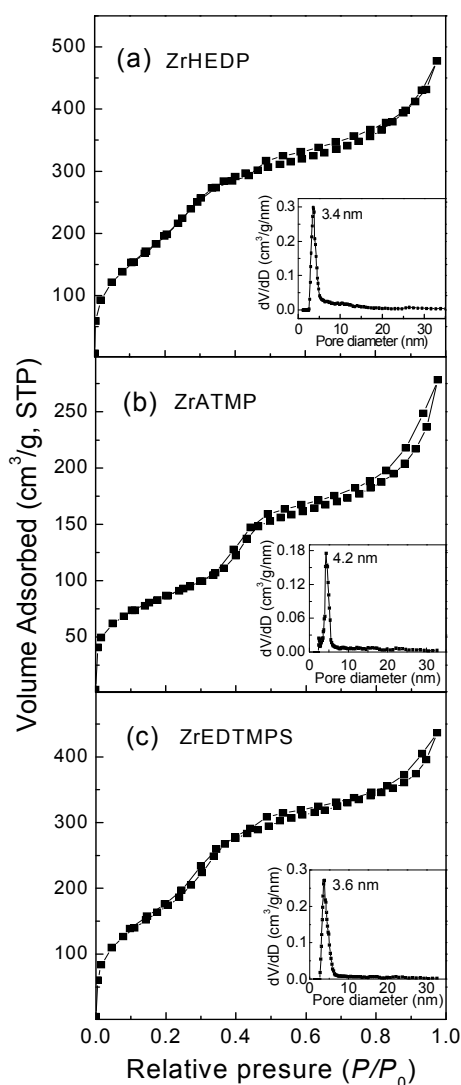


**Fig. 2**  $N_2$  adsorption-desorption isotherms and the corresponding NLDFT pore size distribution curves (*insets*) of the synthesized mesoporous zirconium phosphonates: (a) ZrHEDP, (b) ZrATMP and (c) ZrEDTMPS.

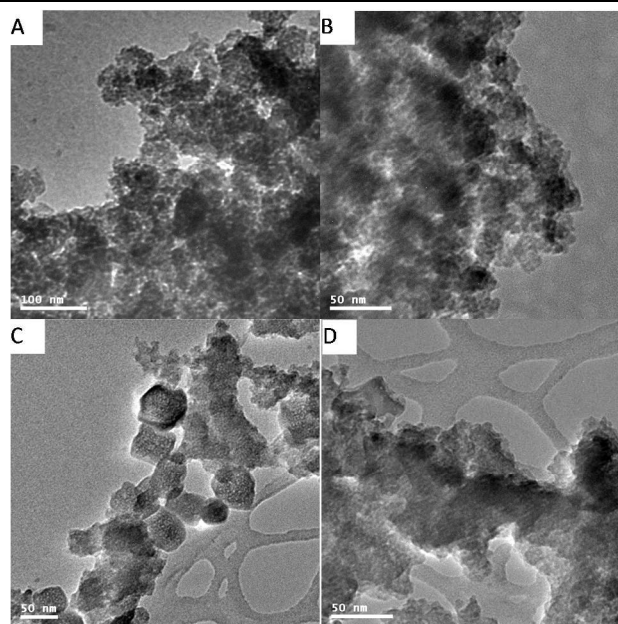


**Fig. 3** TEM images of the synthesized mesoporous zirconium phosphonates: (A) ZrHEDP, (B) ZrATMP, and (C,D) ZrEDTMPS.

The TEM images of the synthesized ZrHEDP, ZrATMP and ZrEDTMPS are shown in Fig. 3. ZrHEDP was assembled by particles with mesopores dispersed fully on each particle (Fig. 3A). ZrATMP was consisted of conglomerated particles as well, but distinct pore channel can be observed with a pore diameter of around 4 nm, demonstrating a short-range order of the mesostructure (Fig. 3B). It is noteworthy that ZrEDTMPS mostly consisted of well dispersed nanoparticles with the sizes of 50–100 nm, and uniform pores in short-range ordered arrangement were through each particle (Figs. 3C and D). Besides, a secondary pore system was generated by the particle assembly for the three samples, consistent with the  $N_2$  adsorption analysis.

Fig. 4 shows the FT-IR spectra of the synthesized ZrHEDP, ZrATMP and ZrEDTMPS, which are similar. In the each spectrum, the strong broad band at  $3400\text{ cm}^{-1}$  and the sharp band at  $1635\text{ cm}^{-1}$  correspond to the surface-adsorbed water and

hydroxyl groups.<sup>35</sup> The bands around 2800–3000  $\text{cm}^{-1}$  and 1450  $\text{cm}^{-1}$  are assigned to the C-H stretching vibration and bending modes, respectively. The band at 1431–1459  $\text{cm}^{-1}$  could be attributed to P-C stretching vibration from organophosphate groups, and the bands at 1333 and 1380  $\text{cm}^{-1}$  are assigned to C-N and C-O stretching vibrations, respectively.<sup>36,37</sup> The weak band at 1150  $\text{cm}^{-1}$  is attributed to P-O asymmetrical stretching vibration from  $\text{RPO}_2(\text{OH})$  groups.<sup>38,39</sup> Besides, the symmetrical stretching modes of the  $\text{O}_3\text{P}$  groups are observed from the strong absorption at 1050  $\text{cm}^{-1}$ ,<sup>40</sup> though this sharp band was attributed to the stretching vibrations of P-O-Zr and as an evidence of the structural formation of zirconium phosphonate.<sup>33</sup> Peaks at 815–821  $\text{cm}^{-1}$  and 570–590  $\text{cm}^{-1}$  are assigned to the framework vibration of Zr-O-P and Zr-O bonds, respectively.<sup>41,42</sup>

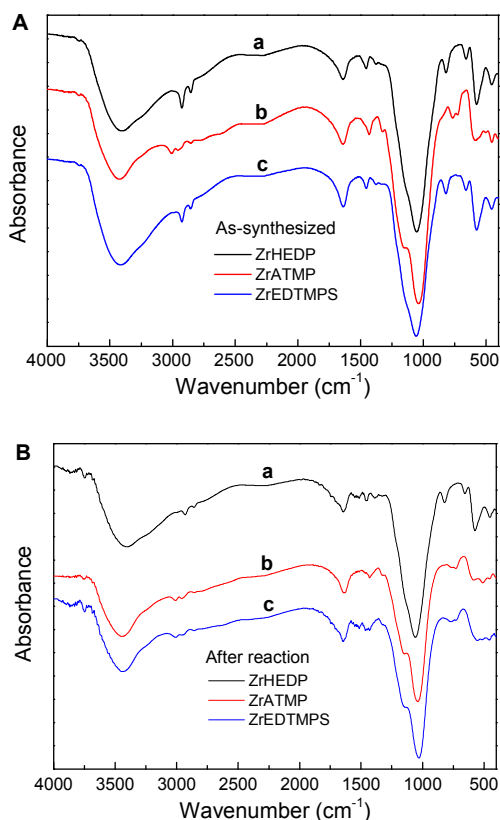


**Fig. 4** FT-IR spectra of (A) the synthesized mesoporous zirconium phosphonates and (B) the samples after four-time recycling in the esterification of cyclohexanol with acetic acid: (a) ZrHEDP, (b) ZrATMP and (c) ZrEDTMPS.

<sup>31</sup>P MAS NMR spectroscopy was conducted to provide useful information on the nature of the phosphonate groups (Fig. 5). It has been reported that the binding of phosphonic acid is primarily through esterification with surface hydroxyls of zirconium oxide.<sup>43</sup> The mono- and bidentate species of phosphonic acid coupled on  $\text{ZrO}_2$  could be expected to have chemical shift towards upfield ranging between 5 and 15 ppm from the free acid,<sup>44,45</sup> while the <sup>31</sup>P chemical shift of the free ligand HEDP is located at  $\delta = 19.5$  ppm.<sup>46</sup> A main resonance signal centered at  $\delta = 12.2$  ppm with a shoulder peak at  $\delta = 3.8$  ppm was observed in the <sup>31</sup>P spectrum of ZrHEDP, which is in the range characteristic of phosphonates.<sup>26,37,47,48</sup> The resonance signal at  $\delta = 12.2$  ppm

could be assigned to the organic phosphorus species connected to zirconium in the form of  $\text{RPO}_2(\text{OH})$ , which could further condense with Zr-OH to form  $\text{RPO}_3$  exhibiting signal at  $\delta = 3.8$  ppm.<sup>26</sup> ZrEDTMPS provided similar curve as that of ZrHEDP, with the resonances at  $\delta = 13.6$  ppm and 2.6 ppm corresponding to  $\text{RPO}_2(\text{OH})$  and  $\text{RPO}_3$  connectivities, respectively. A broad peak between 0–20 ppm was observed for ZrATMP, indicating an intricate phosphorus species including  $\text{RPO}_2(\text{OH})$  and  $\text{RPO}_3$  together existed in the sample.<sup>49</sup> The change of phosphorus environment in the hybrid materials indicates the formation of P-O-Zr bonds, consistent with the result from FT-IR. And no  $\text{RPO}(\text{OH})_2$  species were observed on mesoporous zirconium organophosphonates, suggesting the integration of organic moieties in the hybrid framework but not pendent on the pore wall.

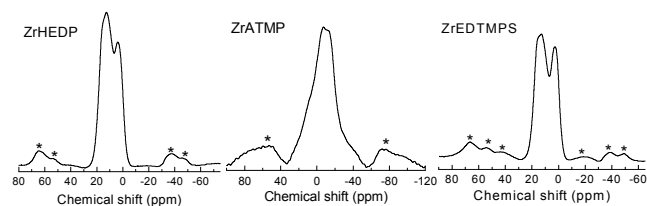


**Fig. 5** <sup>31</sup>P MAS NMR spectra of the synthesized mesoporous zirconium phosphonate materials. Spinning sidebands which appeared corresponding to multiples of the spinning rate are indicated by asterisks.

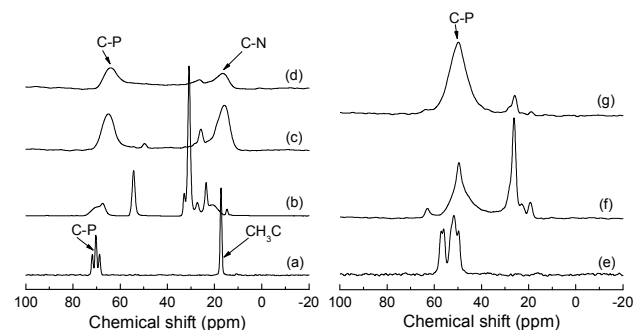


**Fig. 6** <sup>13</sup>C CP/MAS NMR spectra of (a) pure HEDP, (b) surfactant-contained and (c) surfactant-extracted ZrHEDP, (d) surfactant-extracted ZrEDTMPS, (e) pure ATMP, (f) surfactant-contained and (g) surfactant-extracted ZrATMP.

Fig. 6 shows the <sup>13</sup>C CP/MAS NMR spectra for mesoporous zirconium organophosphonate samples. In comparison with HEDP and the as-synthesized sample without surfactant-removal, ZrHEDP exhibited two main signals at  $\delta = 15.8$  and 64.9 ppm (Fig. 6c), which correspond to the carbon atom of the terminal  $\text{CH}_3$  group<sup>47</sup> and the quaternary carbon atom connected to the P=O group of the phosphonate,<sup>50</sup> respectively, suggesting the HEDP groups were dispersed homogeneously within the ZrHEDP network. Due to the coordination of diposphonic acid with zirconium, these two signals broadened, and a downfield shift of about 5 ppm was observed for the resonance at  $\delta = 64.9$  ppm when compared with HEDP. Two other weak peaks at  $\delta = 49.7$  and 25.7 ppm were associated with C atoms of the residual CTAB in the pores.<sup>51</sup> In the <sup>13</sup>C spectrum of ZrEDTMPS (Fig. 6d), two strong peaks at  $\delta = 64.0$  and 16.1 ppm were ascribed to the carbon atoms in nitrilemethylenephosphonate groups and the bridged  $-(\text{CH}_2)_2-$  groups, respectively, and a weak peak at  $\delta =$

26.4 ppm was from the carbon atoms of residual CTAB. As to ZrATMP, the resonance at  $\delta = 49.7$  ppm corresponds to the carbon atoms in the nitrilomethylenephosphonate groups (Fig. 6g), which is 8 ppm downfield shift in comparison with pure ATMP due to the connectivity of phosphonic acid with zirconium. Also the weak resonance of the residual surfactant was observed at  $\delta = 25.7$  and 19.2 ppm. It thus can be deduced from the FT-IR and NMR spectroscopic results that mesoporous zirconium phosphonate materials with organophosphonate groups integrated intactly in the hybrid framework were successfully achieved, though a small amount of CTAB retained in the pore channels.

The  $\text{RPO}_2(\text{OH})$  groups on the surface of ZrHEDP, ZrATMP and ZrEDTMPS could be the acid site provider, and are able to exchange protons with other cationic species, responsible for the  $\text{H}^+$  exchange capability and acid catalysis of zirconium organophosphonate samples.<sup>44</sup> The acid densities of the synthesized zirconium organophosphonate samples were determined by titration with 0.05 M NaOH solution, and listed in Table 2. ZrHEDP has the  $\text{H}^+$  exchange capacity of 1.92 mmol/g, a little larger than ZrATMP (1.25 mmol/g) and ZrEDTMPS (1.42 mmol/g). However, as to the as-synthesized hybrid samples without removal of surfactant, almost no  $\text{H}^+$  exchange capacity was observed, indicating the absence of the  $\text{RPO}_2(\text{OH})$  species that could be generated during acidic ethanol extraction process probably through a transformation of  $\text{P-O}^+\text{CTA}^+$  to P-OH. This also evidenced the mechanistic rationality of the acidic ethanol extraction process for the removal of surfactant species in the pore channels of mesostructured zirconium phosphonates.<sup>52</sup> Furthermore, the acid strength of the synthesized mesoporous zirconium phosphonates was measured by the Hammett indicator method with the use of anthraquinone and 2,4,6-trinitroaniline, and a moderate-to-strong acid strength with  $\text{H}_0$  in the range of -8.2 to -10.10 was observed.<sup>53</sup> Thus, the synthesized mesoporous zirconium organophosphonates can be as promising solid acid catalysts.

The thermostability of the synthesized mesoporous zirconium phosphonate materials was measured by TGA-DTG. The TGA profiles of the samples ZrHEDP, ZrATMP and ZrEDTMPS exhibit mainly three-step weight loss at room temperature–200 °C, 200–400 °C and 400–600 °C (Fig. S1, ESI†), which are assigned to the desorption of water, decomposition of organophosphonate groups and the residual CTAB species, and the further combustion of residual coke, respectively.<sup>37,54</sup> This confirms that the synthesized zirconium phosphonate materials with bridged organic groups are thermally stable over 200 °C. And such thermostability of ZrHEDP, ZrATMP and ZrEDTMPS is high enough for a number of organic-related reactions. Since the surface hydrophilic-hydrophobic property of solid catalysts affected much on their catalytic activity for water-related organic reactions, the water adsorption capacity of the synthesized zirconium phosphonate materials can be measured by assuming the amount of water desorption from TGA as water adsorption capacity, and used to evaluate their surface hydrophilic-hydrophobic property. The amount of weight loss under 200 °C was 12.4%, 9.2% and 7.9% for ZrHEDP, ZrATMP and ZrEDTMPS, respectively. This means the surface hydrophobicity among these three catalysts is  $\text{ZrHEDP} < \text{ZrATMP} <$

ZrEDTMPS, which is consistent with the length of internal organic groups integrated in the hybrid framework, indicating that the introduction of organic groups by selecting appropriate organophosphonates is helpful to adjust the hydrophilic-hydrophobic property of the resultant porous material.

### 3.2 Catalytic activity

In order to test the acid-catalytic performance of mesoporous zirconium organophosphonates in water-related reactions, the esterifications of acetic acid with ethanol and cyclohexanol (about 7 wt% of water was produced when the conversions of the two esterifications reached 100 %) and the ethyl acetate hydrolysis in aqueous solution were performed. For comparison, two conventional solid acids, commercial resin NKC-9 and inorganic  $\text{ZrPO}_4$ , were also tested as catalyst. The catalytic results over various acid catalysts were also summarized in Table 2.

In the esterification of acetic acid with ethanol, after reaction of 5 h, the yield of ethyl acetate over ZrHEDP was 67.5%, a little larger than that of ZrATMP (52.6%) and ZrEDTMPS (66.9%), which is consistent with the tendency of the  $\text{H}^+$  exchange capacity of the mesoporous zirconium phosphonates (Table 2). While the ion-exchange resin NKC-9 exhibited very high initial catalytic performance with the ethyl acetate yield of 88.1%, which is in accordance with its large  $\text{H}^+$  exchange capacity of 4.3 mmol/g.  $\text{ZrPO}_4$  also displayed comparable catalytic activity with yield of 54.3% in the esterification of acetic acid with ethanol, due to its high acid content (2.03 mmol/g). Thus, it is deduced that the catalytic activity enhanced with the increase of acid density of the solid catalysts. However, from the point of TOF, it can be seen clearly that mesoporous zirconium phosphonates exhibited much higher catalytic activity than NKC-9 and  $\text{ZrPO}_4$  (Table 2). Furthermore, it is seen from Table 2 that there is a correlation between the TOF values and the surface hydrophobicity (or water adsorption capacity) of the mesoporous zirconium phosphonates. Taking into account of the differences between these catalysts, the high specific surface area and abundant meso-/macroporosity as well as the hydrophobic surface of zirconium organophosphonates are favorable for enhancing the catalytic efficiency of active acid sites and should be responsible for their high TOF values.

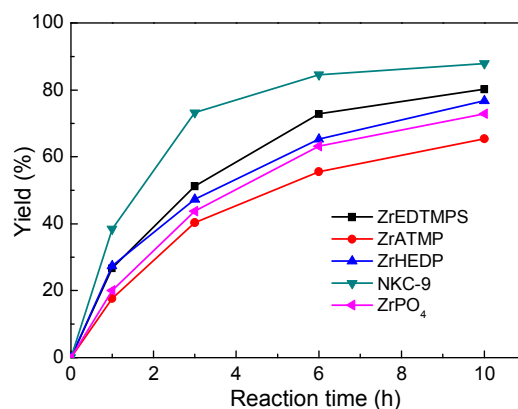


Fig. 8 Dependence of catalytic activities on the time in the esterification of acetic acid with cyclohexanol catalyzed by various catalysts at 100 °C for 10 h.

Fig. 8 shows the dependence of the catalytic activity on the time in the esterification of acetic acid with cyclohexanol over various acid catalysts. At the initial, the reaction rate was fast. After 6 h, it began to slow. NKC-9 showed the fastest reaction rate and reached the cyclohexyl acetate yield of 87.9% after 10 h. ZrHEDP, ZrATMP and ZrEDTMPS exhibited lower reaction rates than NKC-9, with the yields of 76.8%, 65.4% and 75.3% after 10 h, respectively. As to the catalyst ZrPO<sub>4</sub>, 72.9% of cyclohexyl acetate yield was obtained after 10 h of reaction, probably due to its lower specific surface area and poorer porosity in comparison with NKC-9 and mesoporous zirconium phosphonates. Again, from the TOF viewpoint in the esterification of acetic acid with cyclohexanol, the synthesized mesoporous zirconium phosphonates exhibited better catalytic activity than NKC-9 and ZrPO<sub>4</sub> (Table 2). The desirable textural properties and hydrophobic internal organic groups integrated in the hybrid framework should be responsible for their high TOFs. Considering the differences in specific surface areas and porosity, the TOFs among zirconium organophosphonates showed a sequence of ZrEDTMPS > ZrATMP > ZrHEDP, which was consistent with the chain length of corresponding organic groups bridged in organophosphonates. It means that the longer the organic chain length in the hybrid framework is, the stronger the hydrophobicity of the surface for the hybrid mesostructure might be, which favored to drive the reagents to the acid sites and increased their catalytic activity. It is found here that the organic groups integrated in the hybrid framework can also render the hybrid surface hydrophobic and enhanced the catalytic efficiency of active site as the alkyl groups pendent on the inorganic ZrO<sub>2</sub> layer functionalized.<sup>21,22</sup>

**Table 3** Catalytic recycle data in esterification of acetic acid with cyclohexanol over various catalysts.

Samples	Yield (%)			
	1 <sup>st</sup> use	2 <sup>nd</sup> use	3 <sup>rd</sup> use	4 <sup>th</sup> use
ZrHEDP	76.8	78.9	79.6	79.5
ZrATMP	65.4	77.6	78.6	78.7
ZrEDTMPS	75.3	80.2	84.3	84.2
ZrPO <sub>4</sub>	72.9	71.6	71.4	71.4
NKC-9	87.9	82.8	77.6	73.2

In addition to the advantages of easy recovery and separation for a solid catalyst, the other important factors to evaluate a solid catalyst are the simple regeneration and good recyclability. In this work, the used catalysts were regenerated simply by washing with ethanol and drying at 80 °C for next reuse. The results of catalytic recycling of the tested catalysts in esterification of acetic acid with cyclohexanol are summarized in Table 3. After recycling for three times, a slight increase in the yield of cyclohexyl acetate for ZrHEDP, and a prominent increase for ZrATMP and ZrEDTMPS were observed and then kept constant at the fourth time. ZrPO<sub>4</sub> provided the yield almost in constant after the four-time reuse. In contrast, NKC-9 gave a distinct drop in yield from 87.9% for the first recycle to 73.2% at the fourth time. Usually, these results were reasonably related to the changes in the factors such as acidic concentration and textural parameters of the catalysts. The textural parameters for those five catalysts all slightly reduced in comparison with the original samples, which should not be responsible for the increase in yield

(Table 2). Thus, the variation of the acidic concentration of these catalysts should be of great importance for the change of their catalytic activities. After recycling for four times, there was no pronounced diminishment in acidic concentration for ZrPO<sub>4</sub>, but NKC-9 showed a big decrease from 4.33 to 3.49 mmol/g. Interestingly, an apparent increase for ZrHEDP (from 1.92 to 2.0 mmol/g), ZrATMP (from 1.25 to 1.71 mmol/g) and ZrEDTMPS (from 1.42 to 1.58 mmol/g) took place.

In order to explain the change in the acidic concentration for those catalysts, the used catalysts were recovered for FT-IR measurement and the filtrate for ICP analysis. ICP technique was a good and sensitive method to determine the loss of active sites in the reaction solution from catalysts during reaction. After one-time reaction, 0.14 wt% loss of sulfur was detected in the filtrate for NKC-9, and 0.023 wt% and 0.0035 wt% loss of phosphorus for ZrHEDP and ZrPO<sub>4</sub> respectively, but no detectable phosphorus was determined for ZrEDTMPS and ZrATMP. The large loss of active sites for NKC-9 during the reaction is due to the loss of instable sulphonate group via reversible sulphonation in acidic aqueous solution, resulting in the reduction of yield after each use,<sup>55-57</sup> and thus leading to a big drop in acid density from 4.33 to 3.49 mmol/g after four-time reuse. Little loss of phosphorus amount suggests that the P-C bond in organophosphonate was quite stable. And the hydrophobic organic groups for ZrEDTMPS and ZrATMP played an important role in keeping the water molecules out of the inorganic Zr-O-P moieties in the hybrid framework to avoid their decomposition, but the organic groups in HEDP was not hydrophobic enough to avoid their attack by water, thus a leaching of phosphorus happened. The lower loss of phosphorus in ZrPO<sub>4</sub> was probably caused by its more stable four-coordinated P-O-Zr bonds, in comparison with only three P-O-Zr bonds at most for ZrHEDP. The analysis on the loss of active sites can make clear the decrease in yield for NKC-9, but it can not explain the increase in acidic density for zirconium organophosphonates. Anyway, the ICP analysis demonstrates that the active sites of RP-OH species in mesoporous zirconium organophosphonates are much more stable than sulfate species in the ion-exchange resins during water-related acid-catalytic organic reactions.

Furthermore, the recovered mesoporous zirconium phosphonates after four time reuses were measured by FT-IR. As shown in Fig. 4B, in comparison with the fresh catalysts, the recovered ones gave a reduction in the intensities of the peaks at 2858 cm<sup>-1</sup> and 2932 cm<sup>-1</sup> that ascribed to C-H vibrations from CTAB, and an increase in P-O asymmetrical stretching vibration from RPO<sub>2</sub>(OH) groups at 1150 cm<sup>-1</sup>.<sup>38,39</sup> It means the occurrence of the loss of a sprinkle amount of the residual surfactant CTAB occluded in the hybrid materials during reaction at 100 °C between acetic acid and cyclohexanol reactants, with an increase in RP-OH groups. Since part of the organophosphonate species in the hybrid framework of the as-synthesized zirconium phosphonates might electrostatically interact with CTA<sup>+</sup> ions in the form of RPO<sup>-</sup>···CTA<sup>+</sup>, and the surfactant CTA<sup>+</sup> can be removed in acidic ethanol solution with the production of RP-OH groups, here the acetic acid/cyclohexanol mixture acted as acidic alcohol extraction solution, and more P-OH groups generated as the residual CTA<sup>+</sup> ions left. Together with the result obtained from ICP analysis showing no loss of phosphorus for

ZrEDTMPs and ZrATMP, the new generation of P-OH groups for these two recovered samples should be directly associated with the increase in the acidic content, as well as an increase in their catalytic yields. In case of the maintenance of the fourth yield, it should be correlated with the complete loss of CTAB in the first three recycles and no new acid provider was produced at the fourth time. While, the surfactant in ZrPO<sub>4</sub> was completely removed by calcination, and no loss of CTAB happened in reaction, leading to a stable yield for the four recycles. The production of RP-OH species for ZrHEDP during reaction should have an advantage over the loss of phosphorus, therefore a slight increase in acidic concentration was observed, together with its minor increase in catalytic yield of cyclohexyl acetate.

Xiao and co-workers reported the catalytic esterification of cyclohexanol with acetic acid over sulfonated mesoporous polydivinylbenzenes (PDVB-0.1-SO<sub>3</sub>H), giving the conversion of cyclohexanol decreased from 77.5 % to 61.6 % after four recycles.<sup>58</sup> Although the recovered catalyst was activated in 0.1 M H<sub>2</sub>SO<sub>4</sub> after each reuse at room temperature, the reduction of sulfonate acid site could still not be suspended, accompanying with the tailing off of specific surface area and pore volume. Obviously, mesoporous zirconium phosphonates exhibited comparable catalytic activity but better stability than PDVB-0.1-SO<sub>3</sub>H. In addition to the poor recycling result obtained in this work for NKC-9, it can be concluded that sulfonated polymers were not a desirable catalyst for organic acid participated reactions with water as the reactant or product, while mesoporous zirconium phosphonates could be the alternative catalysts for such reactions.

When pure aqueous solution was used as reaction media like in ethyl acetate hydrolysis reaction, the catalytic activities per acidic proton for ZrEDTMPs was the highest (51.1 mmol/mol<sub>acid</sub>/min); ZrHEDP (21.5 mmol/mol<sub>acid</sub>/min) and ZrATMP (30.6 mmol/mol<sub>acid</sub>/min) was in the medium, which was comparable to NKC-9 (35.2 mmol/mol<sub>acid</sub>/min); while tZrPO<sub>4</sub> (15.1 mmol/mol<sub>acid</sub>/min) was the lowest. It is believed that the solid acid catalysts working in water solvent are related to their hydrophobic surfaces.<sup>9,59</sup> The higher activities from mesoporous zirconium phosphonates than that of ZrPO<sub>4</sub> might be due to the more hydrophobic surfaces caused by the bridging organic moieties integrated in the hybrid framework, probably in combination of their high specific surface areas. All above suggest the potential of mesoporous zirconium phosphonates as ideal candidates for water-related reactions.

#### 4. Conclusions

Mesoporous organic-inorganic hybrid zirconium phosphonates (ZrHEDP, ZrATMP and ZrEDTMPs) have been synthesized through a facile surfactant-assisted method, which are water-tolerable solid acids. The organic groups bridged in the phosphonates were integrated in the hybrid framework, and the obtained solids possessed high specific surface areas of 310–749 m<sup>2</sup>/g, uniform pore sizes of 3.4–4.2 nm and large pore volumes of 0.42–0.74 cm<sup>3</sup>/g. When compared with NKC-9 and ZrPO<sub>4</sub>, mesoporous zirconium phosphonates exhibited higher catalytic activities per proton acid active site in hydrolysis of acetyl acetate and higher TOFs for esterification of acetic acid with ethanol / cyclohexanol, due to the combination of their high

specific surface area, abundant mesoporosity, and hydrophobicity of pore surfaces offered by the embedded organic groups in the framework. The hydrophobicity of these three hybrids is in line with the involved alkyl chain length in the sequence of EDTMPS>ATMP>HEDP, and the stronger the hydrophobicity is, the higher the catalytic activity is. A superior recyclability for mesoporous zirconium phosphonates was observed in the esterification of acetic acid with cyclohexanol due to the stable P-C bonds and the hydrophobic hybrid surface, demonstrating the potential of the mesoporous zirconium phosphonates as a new family of important and promising solid acid catalysts for water-related acidic organic reactions.

#### Acknowledgements

This work was supported by the National Natural Science Foundation of China (21073099), the Specialized Research Fund for the Doctoral Program of Higher Education (20110031110016), the Program for Innovative Research Team in University (IRT13022), and the 111 Project (B12015).

#### Notes and references

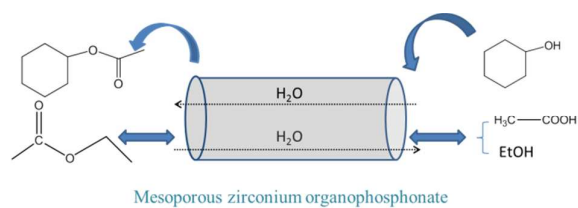
<sup>a</sup> Key Laboratory of Advanced Energy Materials Chemistry (Ministry of Education), Collaborative Innovation Center of Chemical Science and Engineering (Tianjin), College of Chemistry, Nankai University, Tianjin 300071, China. Fax: +86 22 23502604; Tel: +86 22 23509610; E-mail: zyyuan@nankai.edu.cn

<sup>b</sup> School of Chemical Engineering and Technology, Hebei University of Technology, Tianjin 300130, China.

† Electronic Supplementary Information (ESI) available: [Scheme for the material synthesis, TG-DTG analysis]. See DOI: 10.1039/b000000x/

- S.M. Coman, G. Pop, C. Stere, V.I. Parvulescu, J.E. Haskouri, D. Beltrán and P. Amorós, *J. Catal.* 2007, **251**, 388–399.
- J.H. Clark and D.J. Macquarrie, *Chem. Soc. Rev.* 1996, **25**, 303.
- M.G. Clerici, *Topics Catal.* 2000, **13**, 373–386.
- R.B. Wei, Z.Y. Yuan and H.X. Li, *Gazzeta Chimica Italiana* 1997, **127**, 811–813.
- A. Corma and M. Renz, *Angew. Chem. Int. Ed.* 2007, **46**, 298–300.
- A. Corma, M.E. Domine and S. Valencia, *J. Catal.* 2003, **215**, 294–304.
- K. Manabe, S. Limura, X.M. Sun and S. Kobayashi, *J. Am. Chem. Soc.* 2002, **124**, 11971–11978.
- M. Kimura, T. Nakato and T. Okuhara, *Appl. Catal. A* 1997, **165**, 227–240.
- T. Okuhara, *Chem. Rev.* 2002, **102**, 3641–3666.
- S.X. Song and R.A. Kydd, *J. Chem. Soc. Faraday Trans.* 1998, **94**, 1333–1338.
- D.E. López, J.G. Goodwin Jr. and D.A. Bruce, *J. Catal.* 2007, **245**, 381–391.
- H. Chiang and A. Bhan, *J. Catal.* 2010, **271**, 251–261.
- I.V. Kozhevnikov, *Chem. Rev.* 1998, **98**, 171.
- I.V. Kozhevnikov, K.R. Kloetstra, A. Sinnema, H.W. Zandbergen and H. Bekkum, *J. Mol. Catal. A* 1996, **114**, 287.
- P. Madhusudhan Rao, A. Wolfson, S. Kababya, S. Vega and M.V. Landau, *J. Catal.* 2005, **232**, 210–225.
- Y. Kamiya, S. Sakatab, Y. Yoshinaga, R. Ohnishi and T. Okuhara, *Catal. Lett.* 2004, **94**, 45–47.
- Y.P. Zhu, T.Y. Ma, Y.L. Liu, T.Z. Ren and Z.Y. Yuan, *Inorg. Chem. Front.* 2014, **1**, 360–383.
- M. Curini, O. Rosati and U. Costantino, *Curr. Org. Chem.* 2004, **8**, 591–606.
- K. Segawa and T. Ozawa, *J. Mol. Catal. A* 1999, **141**, 249–255.
- Y.L. Liu, Y.P. Zhu, M. Li and Z.Y. Yuan, *Acta Chimica Sinica* 2014, **72**, 521–536.
- D. Lanari, F. Montanari, F. Marmottini, O. Piematti, M. Orrù and L. Vaccaro, *J. Catal.* 2011, **277**, 80–87.

- 22 S. Calogero, D. Lanari, M. Orrù, O. Piermatti, F. Pizzo and L. Vaccaro, *J. Catal.* 2011, **282**, 112-119.
- 23 T.Y. Ma and Z.Y. Yuan, *ChemSusChem* 2011, **4**, 1407-1419.
- 24 Y.P. Zhu, T.Z. Ren and Z.Y. Yuan, *New J. Chem.* 2014, **38**, 1905-1922.
- 25 T.Y. Ma, L. Liu, Q.F. Deng, X.Z. Lin and Z.Y. Yuan, *Chem. Commun.* 2011, **47**, 6015-6017.
- 26 X.Z. Lin and Z.Y. Yuan, *Eur. J. Inorg. Chem.* 2012, 2661-2664.
- 27 U. Ciesla, M. Fröba, G. Stucky and F. Schüth, *Chem. Mater.* 1999, **11**, 227-234.
- 28 P. T. Tanev and T. J. Pinnavaia, *Chem. Mater.* 1996, **8**, 2068.
- 29 M. Kruk and M. Jaroniec, *Chem. Mater.* 2001, **13**, 3169-3183.
- 30 F. Bellezza, A. Cipiciani, U. Costantino and F. Marmottini, *Langmuir* 2006, **22**, 5064-5069.
- 31 X. Shi, J. Liu, C.M. Li and Q.H. Yang, *Inorg. Chem.* 2007, **46**, 7944-7952.
- 32 X. Shi, J.P. Li, Y. Tang and Q.H. Yang, *J. Mater. Chem.* 2010, **20**, 6495-6504.
- 33 Y. Jia, Y. Zhang, R. Wang, J. Yi, X. Feng and Q. Xu, *Ind. Eng. Chem. Res.* 2012, **51**, 12266-12273.
- 34 J. Veliscek-Carolan, T.L. Hanley and V. Luca, *Sep. Pur. Technol.* 2014, **129**, 150-158.
- 35 T.Z. Ren, Z.Y. Yuan and B.L. Su, *Chem. Phys. Lett.* 2003, **374**, 170-175.
- 36 X.J. Zhang, T.Y. Ma and Z.Y. Yuan, *J. Mater. Chem.* 2008, **18**, 2003-2010.
- 37 X.J. Zhang, T.Y. Ma and Z.Y. Yuan, *Eur. J. Inorg. Chem.* 2008, 2721-2726.
- 38 E.V. Bakhmutova-Albert, N. Bestaoui, V.I. Bakhmutov, A. Clearfield, A.V. Rodriguez and R. Llavona, *Inorg. Chem.* 2004, **43**, 1264-1272.
- 39 F. Odobel, B. Bujoli and D. Massiot, *Chem. Mater.* 2001, **13**, 163-173.
- 40 C. Jacopin, M. Sawicki, G. Plancque, D. Doizi, F. Taran, E. Ansoborlo, B. Amekraz and C. Moulin, *Inorg. Chem.* 2003, **42**, 5015-5022.
- 41 J.D. Kim, T. Mori and I. Honma, *J. Power Sources* 2007, **172**, 694-697.
- 42 J.D. Kim, T. Mori and I. Honma, *J. Electrochem. Soc.* 2006, **153**, A508.
- 43 W.A. Schafer, P.W. Carr, E.F. Funkenbusch and K.A. Parson, *J. Chromatogr.* 1991, **587**, 137.
- 44 J. Jiménez-Jiménez, P. Maireles-Torres, P. Olivera-Pastor, E. Rodríguez-Castellón, A. Jiménez-López, D.J. Jones and J. Rozi, *Adv. Mater.* 1998, **10**, 812-815.
- 45 W. Gao, L. Dickinson, C. Grozinger, F.G. Morin and L. Reven, *Langmuir* 1996, **12**, 6429-6435.
- 46 D.R. Jansen, J.R. Zeevaart, Z.I. Kolar, K. Djanashvili, J.A. Peters and G.C. Krijger, *Polyhedron*, 2008, **28**, 1779-1786.
- 47 T. Kimura, *Chem. Mater.* 2003, **15**, 3742-3744.
- 48 T.Y. Ma, X.Z. Lin, X.J. Zhang and Z.Y. Yuan, *Nanoscale* 2011, **3**, 1690-1696.
- 49 C.S. Griffith, M.D.L. Reyes, N. Scales, J.V. Hanna and V. Luca, *ACS Appl. Mater. Interfaces* 2010, **2**, 3436-3446.
- 50 T.Y. Ma and Z.Y. Yuan, *Chem. Commun.* 2010, **46**, 2325-2327.
- 51 H. Nur, L.C. Guan, S. Endud and H. Hamdan, *Mater. Lett.* 2004, **58**, 1971-1974.
- 52 X.Z. Lin and Z.Y. Yuan, *RSC Adv.* 2014, **4**, 32443-32450.
- 53 X. Mo, D.E. López, K. Suwannakan, Y. Liu, E. Lotero, J.G. Goodwin Jr, and C. Lu, *J. Catal.* 2008, **254**, 332.
- 54 T.Y. Ma, X.Z. Lin and Z.Y. Yuan, *J. Mater. Chem.* 2010, **20**, 7406-7415.
- 55 C. Vogel, J. Meier-Haack, A. Taeger and D. Lehmann, *Fuel cells* 2004, **4**, 320-327.
- 56 F. Kučera and J. Jančář, *Polym. Eng. Sci.* 1998, **38**, 783-792.
- 57 N. Shibuya and R. S. Porter, *Macromolecules*, 1992, **25**, 6495-6499.
- 58 F.J. Liu, X.J. Meng, Y.L. Zhang, L.M. Ren, F. Nawaz and F.S. Xiao, *J. Catal.* 2010, **271**, 52-58.
- 59 L. Li, Y. Yoshinaga and T. Okuhara, *Phys. Chem. Chem. Phys.* 1999, **1**, 4913.



Mesoporous zirconium phosphonate materials were fabricated as efficient water-tolerable solid acid catalysts.